ACS APPLIED MATERIALS & INTERFACES

Research Article

Tunable Photomechanics in Diarylethene-Driven Liquid Crystal Network Actuators

Markus Lahikainen, Kim Kuntze, Hao Zeng,* Seidi Helantera, Stefan Hecht, and Arri Priimagi*

Cite This: *ACS Appl. Mater. Interfaces* 2020, 12, 47939−47947

Read Online

ACCESS | Metrics & More | Article Recommendations | Supporting Information

ABSTRACT: The response of soft actuators made of stimuli-responsive materials can be phenomenologically described by a stimulus-deformation curve, depicting the controllability and sensitivity of the actuator system. Manipulating such stimulus-deformation curve allows fabricating soft microrobots with reconfigurable actuation behavior, which is not easily achievable using conventional materials. Here, we report a light-driven actuator based on a liquid crystal polymer network containing diarylethene (DAE) photoswitches as cross-links, in which the stimulus-deformation curve under visible-light illumination is tuned with UV light. The tuning is brought about by the reversible electrocyclization of the DAE units. Because of the excellent thermal stability of the visible-absorbing closed-form DAEs, the absorbance of the actuator can be optically fixed to a desired value, which in turn dictates the efficiency of photothermally induced deformation. We employ the controllability in devising a logical AND gate with macroscopic output, i.e., an actuator that bends negligibly under UV or visible light irradiation, but with profound shape change when addressed to both simultaneously. The results provide design tools for reconfigurable microrobotics and polymer-based logic gating.

KEYWORDS: liquid crystal polymer network, photoactuation, diarylethene, photoswitch, logic gate, reconfiguration
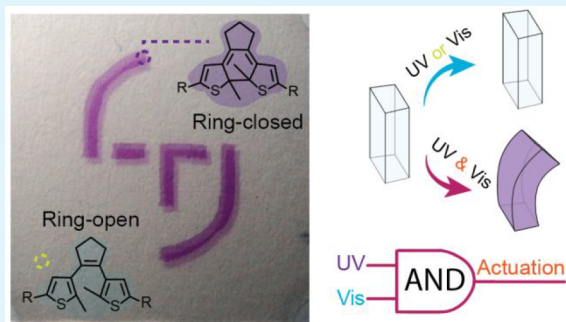
INTRODUCTION

Soft robotics is a research frontier dedicated to combine the flexibility of soft materials with the accurate control inherent to conventional rigid-bodied robots, anticipated to provide technological breakthroughs for human-friendly interfaces, controlled locomotion, and bioinspired robotic adaptation.[1] To apply the soft robots in single-cell manipulation, drug delivery/release, or microfluidics, their size has to be miniaturized.[2] For this, stimuli-responsive materials are often adopted,[3,4] allowing to activate robotic movements wirelessly using heat, magnetic or electric fields, humidity, or light.[5−9] Among the different classes of stimuli-responsive materials, light-driven liquid crystal polymer networks (LCNs) stand out due to their large shape-changes, versatile control over deformation (e.g., bending, coiling, and twisting), easy scalability from centimeter down to micrometer size, and high spatial and temporal resolution of the light activation.[10,11] Conventionally, the light-fueled actuation of LCNs is triggered by photoswitchable molecules incorporated into the polymer network.[12,13] Upon photon absorption, the photoswitches undergo reversible shape changes and induce disorder into the initially ordered polymer network, yielding photochemically induced macroscopic actuation.[14,15] An attractive alternative to trigger actuation is the use of the photothermal effect, i.e., the molecular disorder created by heat released during non-radiative relaxation of photoexcited moieties.[16−19] In the past

decade, many photothermally fueled LCN robotic movements have been demonstrated, including 3D kirigami/origami devices,[20] light steering motion by walking[21] and swimming,[22] object manipulation through gripping,[23,24] and self-sustainable oscillation.[25−27]

The inputs required by an operational actuator are control signal and powering source. For instance, the actuation force or displacement of an electromechanical actuator is controlled through current/voltage input.[28] In light-driven LCN robotics, the actuator performance is dictated by a complex interplay between molecular-level events (e.g., light absorption) and macroscopic properties of the polymer network (elastic modulus and alignment anisotropy).[29,30] For photothermal actuators, the performance can be described by an intensity-deformation curve, as schematically illustrated in Figure 1a. Increasing the illumination intensity increases the amount of deformation of the actuator, which in combination with predesigned shape morphing provides accurate light controllability over the robotic movements.[31] Typically, the intensity-
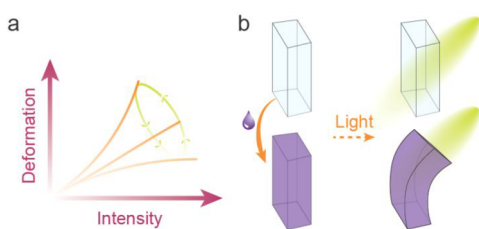
Figure 1. Concept of tunable photomechanics. (a) Performance of a photothermal actuator is described with a light intensity-deformation curve, and modification of the curve profile with an external stimulus allows reconfiguring the light response of the actuator. (b) Schematics of a reprogrammable photothermal actuator that shows minimal deformation initially and exhibits profound shape changes after color change (increased absorption).

deformation curve is fixed during the fabrication process; that is, a conventional photoactuator is responsive yet not reconfigurable. A possibility to tune the light response after fabrication allows reprogramming the performance of the actuator at will, paving way toward design strategies for reconfigurable and adaptive soft robotics.[32]

To manipulate the intensity-deformation curve (i.e., light controllability) and to obtain distinct actuation behavior upon identical light illumination conditions, recent studies have relied on chemical reconfiguration approaches such as the use of dynamic chemical bonds to rearrange the connectivity between polymer chains.[33−37] Only few studies have concentrated on obtaining reconfigurable photoactuation by purely optical methods. The power of optical methods is that in principle they can provide a noncontact reconfigurability platform. However, thus far they lack reversibility over multiple cycles of reconfiguration. For instance, optical de-cross-linking can be used to locally pattern the actuation across an LCN

film, but the obtained effect cannot be easily erased and patterned again.[38] While photochemical excitation allows to reversibly program the actuation behavior, subsequent photothermal actuation resembles the shape-memory effect and only yields few cycles of robotic actuation.[39]

To devise a photothermally driven actuator with light responsivity that can be reversibly tuned, control over light absorption of the photoactuator is the key parameter. By tuning the absorbance, one controls the photosensitivity, i.e., the minimum dose of input energy required for a desired shape change, as illustrated in Figure 1b. Reversible optical modification of absorption can most conveniently be achieved via photochromic molecules.[40,41] The challenge in harnessing photochromic molecules to control photothermal actuation lies in the fact that for the majority of the thus far exploited photochromic moieties—azobenzene[42,43] being the most frequently used—only one of the two states is thermally stable. The lack of bistability leads to inherent thermal relaxation from the metastable to the thermodynamically stable state and thus a continuously changing intensity-deformation relationship. While thermally stable photochromic molecules do exist and *ortho*-fluorinated azobenzenes[44] and hydrozones[45] have been used for bistable photoactuation in LCNs, their absorption changes upon isomerization are often limited. For instance, with an *ortho*-fluorinated azobenzene the absorbance in the visible range may increase upon UV illumination by about 50%,[44] which is insufficient for efficient tuning of the visible-light controllability through changes in material absorption.

Here, we introduce photochromic diarylethene (DAE) cross-links as effective tools toward optically reconfigurable light controllability in photothermal LCN actuators. The DAE units undergo ring-closing and ring-opening via a 6π electrocyclization when illuminated with UV (365 nm) and
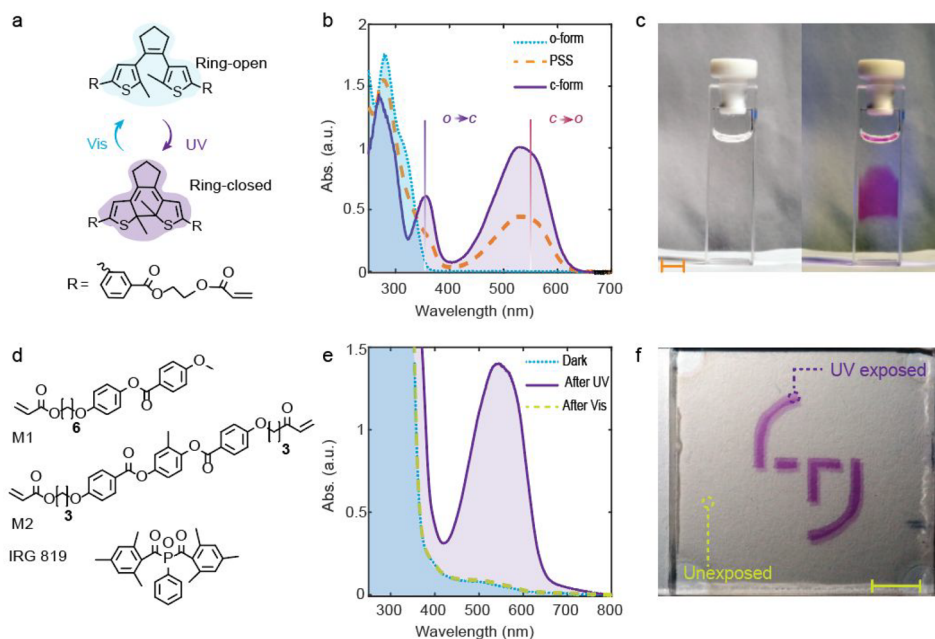

Figure 2. Diarylethene photoswitching. (a) Chemical structures of the ring-open and ring-closed forms of the DAE cross-linker. (b) UV−vis spectra of the DAE cross-linker in a 50 μM acetonitrile solution. (c) Photographs of DAE-containing acetonitrile solution before (left) and after (right) UV illumination. (d) Liquid crystal monomers and photoinitiator used to form LCN soft actuator. (e) UV−vis spectra of the DAE-LCN film before and after electrocyclization. UV: 365 nm, 50 mW cm^{-2}; vis.: 550 nm, 285 mW cm^{-2}. (f) Photograph of the DAE-LCN film after masked exposure to UV light. Scale bars: 5 mm.

visible light (550 nm), respectively, providing a convenient way to selectively address each switching state, i.e., ring-open and ring-closed DAE. Due to the outstanding thermal stability of the ring-closed DAE, the absorbance around 550 nm can be fixed to any value between 0.05 and 1.4 in a 20 μm LCN actuator strip. Hence, we make use of a control signal (UV irradiation) to tune the sensitivity of actuation to the powering source (visible-light irradiation). The DAE-based LCN (DAE-LCN) actuator exhibits AND gate logics: deformation is negligible when exposed only to UV or visible irradiation but pronounced shape changes are observed when exposed to both simultaneously.

RESULTS

Diarylethene Photoswitch. The DAE photoswitch used as the light-absorbing unit in the present study is shown in Figure 2a. It undergoes reversible open → closed ($o-c$) as well as closed → open ($c-o$) interconversion when illuminated with UV and visible light, respectively. As shown in Figure 2b, the open form absorbs strongly in the UV region while the closed form exhibits a band in the visible, centered at $\lambda = 540$ nm, leading to a significant color change from transparent to purple under UV irradiation (Figure 2c). The electrocyclization was studied with ^{1}H NMR, which under 365 nm irradiation yielded a photostationary state (PSS) consisting ca. 56% of the closed-form DAE, the quantum yield (QY) for the $o-c$ conversion being $\Phi_{o\to c} = 0.54$. By irradiating the solution with 550 nm, $c-o$ electrocyclization occurs and the process can be driven to completion, yet with a very low QY of $\Phi_{c\to o} = 0.009$. The low QY of the ring-opening ascompared to the ring-closure is expected,[46] and in fact works for our benefit for maintaining the visible light actuation, as will be discussed later. Further details on the QY determination are given in the Supporting Information.

The core of the DAE molecules was extended with aryl groups, which serve to extend the conjugation and hence shift the absorption of the open as well as closed forms to higher wavelengths and enhance the rigidity of the DAE molecules, rendering them compatible with the polymerizable liquid crystal mixture constituting the actuator (Figure 2d).[47] The two acrylate groups attached to the DAE ensure their covalent attachment to the polymer network during photopolymerization. Details of the DAE synthesis and LCN sample preparation procedure are given in the Supporting Information and the Experimental Methods section, respectively. The electrocyclization of DAE is well preserved in the LCN: UV illumination enhances the absorption in the visible range (Figure 2e) and colorizes the exposed area in purple (Figure 2f). No photodegradation was observed for at least ten cycles of UV/visible irradiation (Figure S1). More details on the light-induced spectral changes and their kinetics in the LCN film are given in Figure S2. The polarized optical micrographs (Figure S3) reveal high homogeneity of the LCN, indicating no disruption of liquid crystalline alignment after incorporating the DAE into the network.

Spectral Stability. The temporal stability of the closed-form, visible-absorbing DAE, was investigated by monitoring the absorbance at 550 nm from a 10 μm thick LCN film containing 5 mol % of DAE at different temperatures (Figures 3a and S4). The half-life was estimated to be over 400 days at room temperature, which is 3 orders of magnitude longer than the *cis*-lifetime of typical azobenzene cross-linkers used in LCNs (Figure S5). The thermal stability decreases at elevated
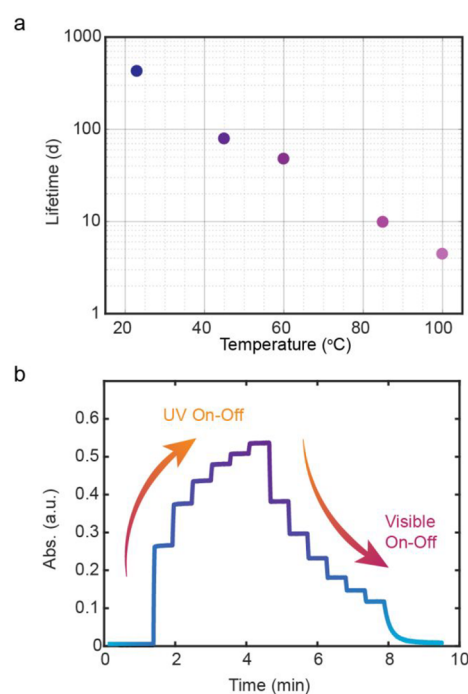

Figure 3. Spectral stability. (a) Thermal lifetime of the ring-closed DAE at different temperatures, measured for a 10 μm DAE-LCN film. (b) Stepwise change of absorbance (at 550 nm) in the DAE-LCN film by sequential irradiation with UV and visible light. UV: 365 nm, 120 mW cm^{-2}, 2 s; vis.: 550 nm, 300 mW cm^{-2}, 2 s.

temperatures, but even at 100 °C, the lifetime of the closed form exceeds 4 days (Figure 3a). Hence, the DAE-based LCN can be considered as a bistable system whose spectral properties can be purely controlled via optical excitations. This allows the absorbance to be fixed to a desired level, as demonstrated in Figure 3b where the LCN was periodically illuminated with UV irradiation, yielding a stepwise increase in the absorbance at 550 nm, whereas subsequent illumination at this wavelength allows controlled decrease in the absorbance in a similar stair-like fashion. This feature is not only useful for photomechanical actuation, but potentially also for applications in tunable photonics.[48]

Light-Tunable Photomechanics. For the photomechanical actuation studies, we fabricated a DAE-LCN actuator with $3 \times 0.5 \times 0.02$ mm^3 dimensions and 90° twisted molecular alignment. A tip-end bending angle is used to quantify the mechanical response under different irradiation conditions, as shown in the inset of Figure 4a. The bending is due to anisotropic thermal expansion within the strip, dictated by the molecular alignment and independent from the incident light direction.[49] Such bending occurs within the temperature range much below the nematic−isotropic phase transition of the LCN material, which is observed above 150 °C (Figure S6). Different molecular alignment or cutting direction would lead to different shape morphing such as twisting, coiling or contraction.[50] Bending-type deformation was chosen because it is easy to characterize by simply measuring the bending angle under different illumination conditions. We note also that the initial state of the actuator is bent, which is due to residual stress in the LCN generated during photopolymerization at elevated temperature.[51] Further details on the actuator fabrication are given in Experimental Methods, and a
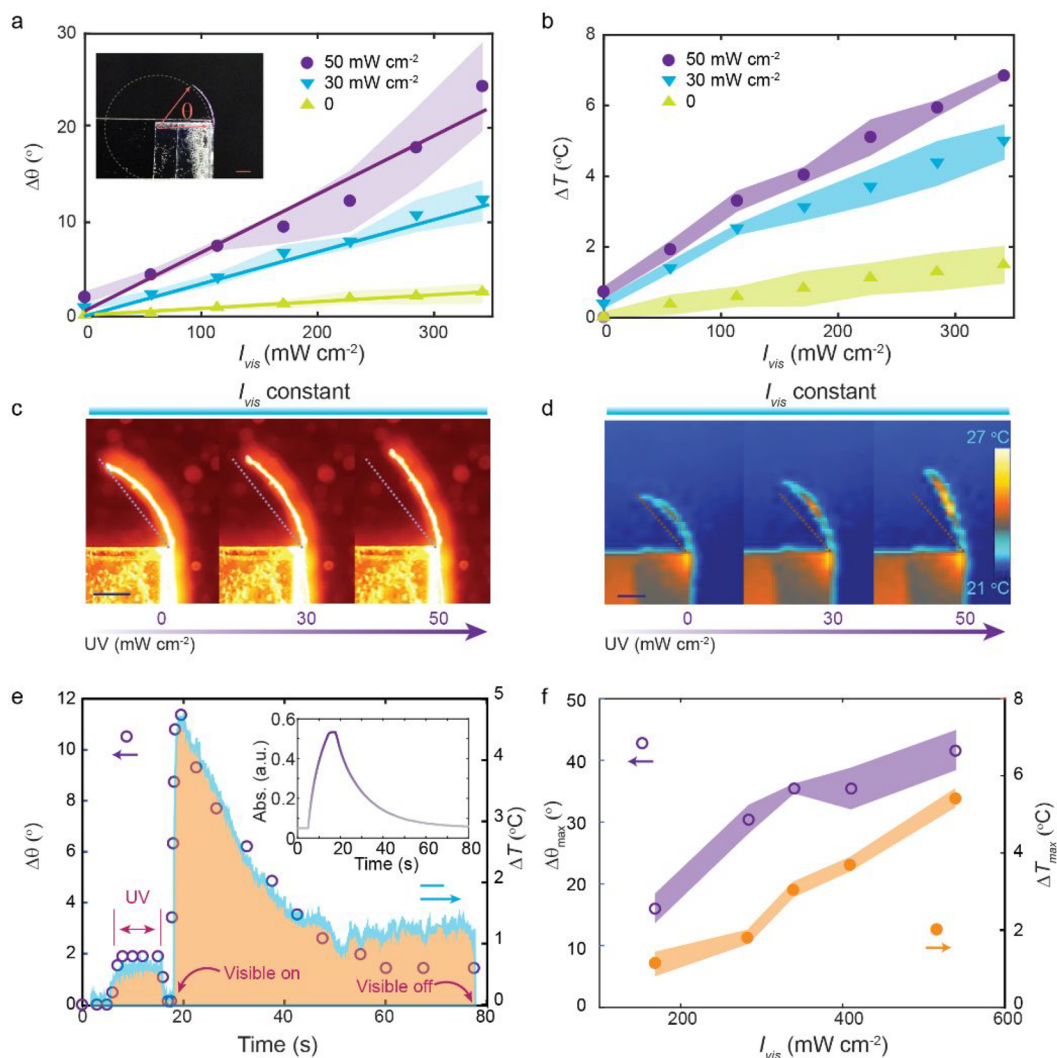
Figure 4. Light-tunable photomechanics. (a) Bending angle of the DAE-LCN strip upon irradiation with UV and visible light with different intensities. The sensitivity of the actuator to visible light (550 nm) is estimated from the linear fit to the intensity-deformation (bending) curve. Inset: optical image of the bending strip and indication of the strip bending angle for actuation measurements. (b) Temperature change of the actuator upon irradiation with UV and visible light with different intensities. (c and d) Optical and thermal images of the strip under 285 mW cm^{-2} visible-light illumination using UV exposure of different intensities. (e) Bending angle (purple dots) and temperature change (blue line) of the strip under subsequent illumination with UV (365 nm, 50 mW cm^{-2}, 10 s) and visible (550 nm, 285 mW cm^{-2}) light. Inset shows the corresponding absorbance changes of the strip. (f) Maximum bending angle (purple), and temperature change (orange) induced by different visible-light intensities after an identical UV pre-exposure (365 nm, 50 mW cm^{-2}, 10 s). Error bars in panels a, b, and f indicate standard deviation of $n = 3$ measurements.

schematic drawing of the characterization setup is shown in Figure S7.

The light sensitivity (absorbance) of the DAE-LCN actuator can be controlled by exposure with UV and visible light. As $\Phi_{o \rightarrow c} \gg \Phi_{c \rightarrow o}$, the PSS is rich of ring-closed DAE when applying UV and visible light simultaneously, and visible-light absorption is retained even under relatively strong visible excitation (Figure S2c,d). The intensity-deformation curves under different UV doses are shown in Figure 4a. Without using UV light, the actuator bends moderately under 550 nm, with sensitivity of 7.1° per W cm^{-2} (Figure 4b, green). The small deformation is due to small absorption ($A \approx 0.05$) of the ring-open DAE at 550 nm (Figure 2e). Even a small dose of UV significantly enhances the visible-light absorption and as a result, the deformation of the strip is boosted, the efficiency being 34.1° per W cm^{-2} and 62° per W cm^{-2} using UV

exposure of 30 mW cm^{-2} (Figure 4a, blue) and 50 mW cm^{-2} (Figure 4a, purple), respectively. We emphasize that the deformation under visible-light irradiation is due to the photothermal effect, driven by the closed-form DAE absorbing the photons, transferring the photon energy to heat, and subsequently triggering the actuation of the LCN. The photothermally induced temperature increase is shown in Figure 4b and the optical and thermal camera images of the actuator in Figure 4c,d.

We note that UV irradiation alone induces neither photothermal nor photochemical actuation. For example, UV exposure of 50 mW·cm^{-2} brings only 2° bending and <1 °C temperature elevation. This is explained by the high $\Phi_{o \rightarrow c}$, driving the $o-c$ electrocyclization rather than converting light energy to heat. The absence of photochemical actuation (see Figure S8), different from the diarylethene-based photo-

chemical actuator reported by the Ikeda group,[52] is attributed to negligible shape change between the open-form and closed-form DAE[53] and to moderate concentration (5 mol %) of the DAE units. Different to many azobenzene-containing LCNs,[54−56] the Young's modulus of the DAE-LCN (~1.3 GPa at room temperature) was not affected by the electro-cyclization and the stress−strain behavior remains unchanged before and after UV illumination (Figure S9). Hence, in our actuator UV light acts as the "control signal" to modify the sensitivity of the actuator, while visible light takes the role of the "power source" that initiates the deformation. The mechanical response upon heating the actuator in a water bath (Figure S10a) is stable, as expected based on the thermosensitive nature of LCNs. Upon photothermal heating, the sample deformation reduces slightly over a time span of 60 min (Figure S10b). This may be due to slight degradation of diarylethene units upon moderate-intensity UV illumination (50 mW cm^{-2}).

When the UV and visible light are not applied simultaneously, the actuation is unsteady. Figure 4e shows the bending of the DAE-LCN strip upon sequential UV and visible irradiation. First, UV irradiation (10 s, 50 mW cm^{-2}) is used to raise the absorbance of the LCN from 0.05 to 0.5 (inset of Figure 4e). Then, the UV irradiation is ceased and visible light (550 nm, 285 mW cm^{-2}) is impinged on the strip, which quickly reaches the maximum bending angle (11° bending within 2 s) and then gradually retains the original shape. The photothermally induced deformation is driven by heat equilibrium, and the kinetics (Figure S11) is dictated by the heat capacity of the material. The extent of bending depends on the excitation power and the corresponding photoinduced temperature increase (Figures 4f and S12). The subsequent relaxation is due to ring-opening of the DAE cross-linker moieties upon visible-light illumination, which constantly reduces the absorption at 550 nm, thus gradually decreasing the photoinduced heating (Figure 4e, blue) and deformation. Exposure to visible-light illumination in the absence of UV leads to gradually decreasing actuation (Figure S13). Herein, pronounced differences between simultaneous and sequential UV−visible excitation can be observed. Upon simultaneous illumination, the population of the o- and c-forms of DAE reach an equilibrium, which stabilizes the actuation to a certain level (Figures 4a and S2d). Upon sequential illumination, the drop of absorption caused by visible-light excitation leads to continuous decrease in deformation (Figure 4e). We would like to note that rather than being a drawback, the dual wavelength dependence is a characteristic of the DAE-based LCN actuator which, as shown next, enables a proof-of-principle application of logical gating in photoactuation.

AND-Gate Photoactuation. Figure 5a shows the photo-induced bending under simultaneous UV (0 to 60 mW·cm^{-2}) and visible-light (0 to 342 mW·cm^{-2}) illumination. When the intensity of either of the irradiation sources is increased, the bending is boosted. On the other hand, if either of the irradiation sources is removed, the bending is negligible. Such behavior resembles the AND-gate logic, where an output signal is provided only when both input signals are applied simultaneously. In our notation the two light sources act as the input signals, while the deformation serves as the output. The AND logical table can be constructed as follows (Figure 5b): (1) If no light is applied, the DAE-LCN remains transparent and no heat is generated, hence no actuation; (2) when only UV light is used, the DAE-LCN becomes absorbing
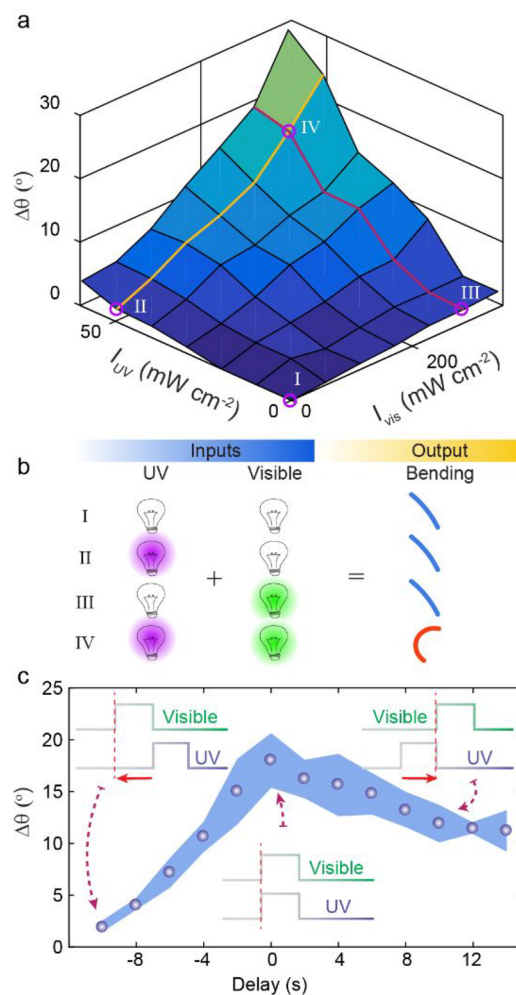

Figure 5. AND-gate photoactuation. (a) Bending angle of the DAE-LCN as a function of UV and visible light intensities. The numbers indicate the different gating status shown in panel b. (b) Logic table of the AND-gate photoactuator, the two inputs being the UV and Vis irradiation and the output being the bending of the strip. (c) The maximum bending of the strip upon changing the delay between UV and visible exposures. The error bar indicates standard deviation of n = 3 measurements.

but no photothermal heating takes place due to the lack of visible-light irradiation, hence no actuation; (3) if only visible light is used, the DAE-LCN remains transparent, hence no actuation (or to be more precise, only very minor actuation is observed); (4) by applying both light inputs simultaneously, the AND-gate is activated and the DAE-LCN deforms.

The bending angle of the AND-gate photoactuator is dictated by the absorbance and resultant photoinduced temperature increase (Figure S14a,b). If the visible-light intensity is kept constant (red line in Figure 5a), an increase in the UV intensity increases the population of closed-form DAE in the PSS, hence boosting the actuation (Figure S14c). By varying the visible-light intensity under constant UV illumination (yellow line in Figure 5a), the photothermal heating is boosted but the absorption of the film decreases as the conversion from the ring-closed to ring-open DAE is enhanced (Figure S14d). We also investigated the dependence of the AND gate actuation on the timing of the two inputs by applying UV light (10 s, 50 mW cm^{-2}) onto the DAE-LCN

and varying the time delay between the UV (10 s, 285 mW cm^{-2}) and visible inputs. The bending angles are recorded instantly after ceasing the visible light, and the results are plotted in Figure 5c. When the visible light precedes the UV input, only minimal actuation is observed as the sample is transparent and cannot absorb light energy. Deformation starts to appear when the two signals overlap, reaching the maximum when there is no delay between the two inputs. When visible light succeeds the UV illumination, the deformation decreases as the ring-opening reaction reduces the absorbance of the LCN in the absence of UV irradiation. When there is no overlap between the signals, the deformation persists as the UV-induced absorption remains due to the stability of closed-form DAE (Figure 3a). These dynamical responses to sequential illuminations could in the future provide a time-wise programming strategy for polymer-based logical circuits.

DISCUSSION

The light-tunable photoactuation presented relies on the photochromic properties of the DAE photoswitch, providing a unique linkage between two light stimuli: UV light is used for controlling the sensitivity (absorption) of the actuator in the visible range whereas visible light is driving shape deformation. Modifying the light absorption of the actuator after polymerization enables reconfigurable actuation where photothermal actuation strength in response to visible irradiation can be tuned. While many photochromic molecules have been used in shape-shifting LCNs,[57−61] they fall short to combine properties provided by the DAE, i.e., excellent thermal stability, large spectral separation of the isomers and thus significant absorption changes upon illumination, and low quantum yield of light-induced back isomerization to the thermodynamically stable state. This unique combination allows us to devise a logical-gate photoactuator using a single photochromic compound only. In addition, please note that the encoding of logical responsiveness can be processed through mask exposure on a 2D material sheet, which may bring opportunities in kirigami/origami-type devices with complex shape-morphing.[34,62]

We highlight once more that, in our system, DAE is used to invoke photothermal actuation. To achieve bistable, photochemically induced actuation, larger concentration of DAE in the LCN should be used, as has been demonstrated earlier.[52] Another versatile strategy for light-induced bistable actuation with DAE is based on single crystals, in which case shape deformation results from the changes in crystal packing caused by electrocyclization.[63,64] However, the AND-gate operation is possible in neither photochemically driven DAE-containing networks nor DAE crystals.

Logic gates and circuits are basic tools in hard-bodied, electronically driven rigid robots. Yet incorporating similar logical operation principles into soft robots is a challenge due to the mismatch between conventional rigid electronic components and compliant bodies.[31] Recently, different logic circuits have been incorporated into soft pneumatic systems leading to complex robotic movement.[65,66] However, the research on photomechanical logic gate -type operations are mostly limited to sol−gel transition of hydrogels,[67−69] where additional inputs (temperature, pH, and electric field) are often needed, increasing the complexity of these systems. The presented fully optically controlled AND-gate photoactuator is unique, and there are multitude of possibilities to extend our concept to other types of logic gates. Future studies may also involve integration between different logic-gate photoactuators to build up polymer-based robots showing more sophisticated behavior than what can be achieved with a single logic-gate photoactuator. This may yield soft robots with automated task execution, taking action only when a combination of stimuli is met, making decisions through the designed logic circuitry. We anticipate that the paradigm of logic gates in the context of photoactuation may broaden the perspective of soft microrobotics and intelligent microdevices.

CONCLUSIONS

We have devised a photothermally driven, diarylethene-based liquid crystal network photoactuator. The exceptional thermal stability of the closed-form diarylethene allows the visible-light absorbance of the actuator to be optically fixed to a desired value via suitable dose of UV irradiation, which acts as a control signal. This, in turn, enables all-optical control over the macroscopic deformation in response to visible light, which acts as the power source for the actuator. The diarylethene-based photoactuator allowed us to devise an AND logical gate with two optical inputs (UV and visible light) and a mechanical output (macroscopic bending). The photomechanical system presented gives new insights to set soft matter in motion via interplay between photochemical and photothermal effects, striving photoactuation toward logical gating and, in the longer term, even logical circuitry. We believe that such intelligent photoactuators may have a variety of applications in soft robotics, photonics and optoelectronics.

MATERIALS AND METHODS

LCN Monomer Mixture Preparation. The LCNs were made by photopolymerization of a mixture containing 72.5 mol % of LC monomer 4-methoxybenzoic acid 4-(6-acryloylox-yhexyloxy)phenyl ester (M1, Synthon Chemicals), 21 mol % of LC cross-linker 1,4-bis-[4-(3-acryloyloxypropyloxy)benzoyloxy]-2-methylbenzene (M2, Synthon chemicals), 5 mol % of diaylethene cross-linker (DAE), and 1.5 mol % of photoinitiator bis(2,4,6-trimethylbenzoyl)-phenylphosphineoxide (IRG 819, Sigma-Aldrich). DAE was synthesized in house (see the synthesis route in the Supporting Information). All other molecules were used as received. The monomer mixture was dissolved in dichloromethane and filtered through PTFE syringe filter (pore size 0.2 μm, Sigma-Aldrich). Finally, the solvent was evaporated at 80 °C for 2 h. The isotropic-to-nematic phase transition temperature of the mixture was ca. 47 °C, as determined with a polarized optical microscope (Zeiss Axio Scope.A1).

Photopolymerization. Glass substrates were cleaned by sonication in acetone and 2-propanol baths, 20 min each. The glass slides were spin coated with 1 wt % water solution of poly(vinyl alcohol) (PVA, Sigma-Aldrich; 4000 rpm, 1 min). Two glass slides were rubbed unidirectionally using satin cloth. Before and after rubbing, the coated glass slides were blown with high-pressure nitrogen gas to remove dust particles. The cells were glued from two glass slides with UV glue (UVS 91, Norland Products Inc., Cranbury, N) mixed with spacer particles (Thermo scientific) to define the cell thickness. The rubbing directions of the alignment layers on the glass slides were aligned to be parallel to form planar LC alignment or perpendicular to form 90° twisted alignment. The mixture was infiltrated into the cell on a heating stage at 70 °C (isotropic) and cooled down to 30 °C (nematic) with a rate of 2 °C min^{-1}. The sample was stabilized for 15 min before photopolymerization by using 11 mW cm^{-2} blue LED (420 nm, LED, Thorlabs, 30 min). After photopolymerization the temperature was elevated to 100 °C and the sample was illuminated with 550 nm light (20 mW cm^{-2} for 5 min), in order to convert the majority of DAE molecules to the ring-open form. The cell was opened, and strip-like LCNs were cut from the film using a blade. The fraction of unreacted monomers was ca. 2.5 wt %, as measured by

weighting the photopolymerized DAE-LCN sample before and after soaking in toluene for 5 min.

Characterization. Absorption spectra and isomerization kinetics were measured in a UV−vis spectrophotometer (Cary 60 UV−vis, Agilent Technologies) equipped with a Peltier-thermostated cell holder for temperature control (accuracy 0.1 °C). The 50 μM DAE-acetonitrile sample was measured in a 1 cm quartz cuvette, while the solid-state sample was a 10 μm thick film with planar alignment or a 20 μm thick film with 90° twisted alignment. Cross-polarized microscope images were taken with Zeiss Axio Scope.A1. An LCN strip with dimensions of $3 \times 0.5 \times 0.02$ mm^3 (90° twisted alignment) was used for studying the photomechanical response upon UV (365 nm) and visible (550 nm) illumination (Prior Scientific multiple LED light source). The light sources used were coupled into a liquid light guide equipped with a collimator lens before illuminating the sample. The intensities were measured in front of the sample position. Photographs and movies were recorded using a Canon 5D Mark III camera with a 100 mm objective lens, and thermal images were taken with an infrared camera (FLIR T420BX) equipped with a close-up (2×) lens. Stress−strain curves were determined by a homemade tensile tester in a 50 μm thick planar film with stretching speed of 0.1 mm s^{-1} and stretching direction in parallel with the LC director.

■ ASSOCIATED CONTENT

Ⓢ Supporting Information

The Supporting Information is available free of charge at https://pubs.acs.org/doi/10.1021/acsami.0c12735.

> Synthesis protocol of DAE cross-linker, photokinetic studies of DAE cross-linker, additional UV−vis spectra and actuation data, and cross polarized optical micrographs (PDF)

■ AUTHOR INFORMATION

Corresponding Authors

Arri Priimagi − *Smart Photonic Materials, Faculty of Engineering and Natural Sciences, Tampere University, FI-33101 Tampere, Finland;* ⓞ orcid.org/0000-0002-5945-9671; Email: arri.priimagi@tuni.fi

Hao Zeng − *Smart Photonic Materials, Faculty of Engineering and Natural Sciences, Tampere University, FI-33101 Tampere, Finland;* ⓞ orcid.org/0000-0002-9150-214X; Email: hao.zeng@tuni.fi

Authors

Markus Lahikainen − *Smart Photonic Materials, Faculty of Engineering and Natural Sciences, Tampere University, FI-33101 Tampere, Finland;* ⓞ orcid.org/0000-0002-4891-5352

Kim Kuntze − *Smart Photonic Materials, Faculty of Engineering and Natural Sciences, Tampere University, FI-33101 Tampere, Finland*

Seidi Helantera − *Smart Photonic Materials, Faculty of Engineering and Natural Sciences, Tampere University, FI-33101 Tampere, Finland*

Stefan Hecht − *Department of Chemistry and IRIS Adlershof, Humboldt-Universität zu Berlin, 12489 Berlin, Germany; DWI-Leibniz Institute for Interactive Materials, 52074 Aachen, Germany; Institute of Technical and Macromolecular Chemistry, RWTH Aachen University, 52074 Aachen, Germany;* ⓞ orcid.org/0000-0002-6124-0222

Complete contact information is available at:
https://pubs.acs.org/10.1021/acsami.0c12735

Author Contributions

A.P., St.H., and H.Z. conceived the project. M.L. carried out experiments with help of Se.H. and K.K., under supervision of H.Z. and A.P. K.K. synthesized the diarylethene molecule under supervision of St.H. M.L., H.Z., and A.P. wrote the manuscript with contributions from all authors. All authors have given approval to the final version of the manuscript.

Notes

The authors declare no competing financial interest.

■ ACKNOWLEDGMENTS

■ REFERENCES

(1) Rus, D.; Tolley, M. T. Design, Fabrication and Control of Soft Robots. *Nature* **2015**, *521*, 467−475.

(2) Nelson, B. J.; Kaliakatsos, I. K.; Abbott, J. J. Microrobots for Minimally Invasive Medicine. *Annu. Rev. Biomed. Eng.* **2010**, *12*, 55−85.

(3) McCracken, J. M.; Donovan, B. R.; White, T. J. Materials as Machines. *Adv. Mater.* **2020**, *32*, 1906564.

(4) Hines, L.; Petersen, K.; Lum, G. Z.; Sitti, M. Soft Actuators for Small-Scale Robotics. *Adv. Mater.* **2017**, *29*, 1603483.

(5) Tottori, S.; Zhang, L.; Qiu, F.; Krawczyk, K. K.; Franco-Obregon, A.; Nelson, B. J. Magnetic Helical Micromachines: Fabrication, Controlled Swimming, and Cargo Transport. *Adv. Mater.* **2012**, *24*, 811−816.

(6) Nocentini, S.; Parmeggiani, C.; Martella, D.; Wiersma, D. S. Optically Driven Soft Micro Robotics. *Adv. Opt. Mater.* **2018**, *6*, 1800207.

(7) He, Q.; Wang, Z.; Wang, Y.; Minori, A.; Tolley, M. T.; Cai, S. Electrically Controlled Liquid Crystal Elastomer-Based Soft Tubular Actuator with Multimodal Actuation. *Sci. Adv.* **2019**, *5*, No. eaax5746.

(8) Davidson, Z. S.; Shahsavan, H.; Aghakhani, A.; Guo, Y.; Hines, L.; Xia, Y.; Yang, S.; Sitti, M. Monolithic Shape-Programmable Dielectric Liquid Crystal Elastomer Actuators. *Sci. Adv.* **2019**, *5*, No. eaay0855.

(9) Chen, X.; Goodnight, D.; Gao, Z.; Cavusoglu, A. H.; Sabharwal, N.; Delay, M.; Driks, A.; Sahin, O. Scaling up Nanoscale Water-Driven Energy Conversion into Evaporation-Driven Engines and Generators. *Nat. Commun.* **2015**, *6*, 7346.

(10) del Barrio, J.; Sánchez-Somolinos, C. Light to Shape the Future: From Photolithography to 4D Printing. *Adv. Opt. Mater.* **2019**, *7*, 1900598.

(11) White, T. J.; Broer, D. J. Programmable and Adaptive Mechanics with Liquid Crystal Polymer Networks and Elastomers. *Nat. Mater.* **2015**, *14*, 1087−1098.

(12) Boelke, J.; Hecht, S. Designing Molecular Photoswitches for Soft Materials Applications. *Adv. Opt. Mater.* **2019**, *7*, 1900404.

(13) Lancia, F.; Ryabchun, A.; Katsonis, N. Life-like Motion Driven by Artificial Molecular Machines. *Nat. Rev. Chem.* **2019**, *3*, 536−551.

(14) Ahn, S. K.; Ware, T. H.; Lee, K. M.; Tondiglia, V. P.; White, T. J. Photoinduced Topographical Feature Development in Blueprinted Azobenzene-Functionalized Liquid Crystalline Elastomers. *Adv. Funct. Mater.* **2016**, *26*, 5819−5826.

(15) Ube, T.; Ikeda, T. Photomobile Polymer Materials with Complex 3D Deformation, Continuous Motions, Self-Regulation, and Enhanced Processability. *Adv. Opt. Mater.* **2019**, 7, 1900380.

(16) Dong, L.; Zhao, Y. Photothermally Driven Liquid Crystal Polymer Actuators. *Mater. Chem. Front.* **2018**, 2, 1932−1943.

(17) Liu, L.; Liu, M. H.; Deng, L. L.; Lin, B. P.; Yang, H. Near-Infrared Chromophore Functionalized Soft Actuator with Ultrafast Photoresponsive Speed and Superior Mechanical Property. *J. Am. Chem. Soc.* **2017**, 139, 11333−11336.

(18) Pilz Da Cunha, M.; Van Thoor, E. A. J.; Debije, M. G.; Broer, D. J.; Schenning, A. P. H. J. Unravelling the Photothermal and Photomechanical Contributions to Actuation of Azobenzene-Doped Liquid Crystal Polymers in Air and Water. *J. Mater. Chem. C* **2019**, 7, 13502−13509.

(19) Zhang, H.; Mourran, A.; Möller, M. Dynamic Switching of Helical Microgel Ribbons. *Nano Lett.* **2017**, 17, 2010−2014.

(20) Verpaalen, R. C. P.; Pilz da Cunha, M.; Engels, T. A. P.; Debije, M. G.; Schenning, A. P. H. J. Liquid Crystal Networks on Thermoplastics: Reprogrammable Photo-Responsive Actuators. *Angew. Chem., Int. Ed.* **2020**, 59, 4532−4536.

(21) Zuo, B.; Wang, M.; Lin, B. P.; Yang, H. Visible and Infrared Three-Wavelength Modulated Multi-Directional Actuators. *Nat. Commun.* **2019**, 10, 4539.

(22) Palagi, S.; Mark, A. G.; Reigh, S. Y.; Melde, K.; Qiu, T.; Zeng, H.; Parmeggiani, C.; Martella, D.; Sanchez-Castillo, A.; Kapernaum, N.; Giesselmann, F.; Wiersma, D. S.; Lauga, E.; Fischer, P. Structured Light Enables Biomimetic Swimming and Versatile Locomotion of Photoresponsive Soft Microrobots. *Nat. Mater.* **2016**, 15, 647−653.

(23) Wani, O. M.; Zeng, H.; Priimagi, A. A Light-Driven Artificial Flytrap. *Nat. Commun.* **2017**, 8, 15546.

(24) Lu, X.; Zhang, H.; Fei, G.; Yu, B.; Tong, X.; Xia, H.; Zhao, Y. Liquid-Crystalline Dynamic Networks Doped with Gold Nanorods Showing Enhanced Photocontrol of Actuation. *Adv. Mater.* **2018**, 30, 1706597.

(25) Serak, S.; Tabiryan, N.; Vergara, R.; White, T. J.; Vaia, R. A.; Bunning, T. J. Liquid Crystalline Polymer Cantilever Oscillators Fueled by Light. *Soft Matter* **2010**, 6, 779−783.

(26) Zeng, H.; Lahikainen, M.; Liu, L.; Ahmed, Z.; Wani, O. M.; Wang, M.; Yang, H.; Priimagi, A. Light-Fuelled Freestyle Self-Oscillators. *Nat. Commun.* **2019**, 10, 5057.

(27) Gelebart, A. H.; Vantomme, G.; Meijer, B. E. W.; Broer, D. J. Mastering the Photothermal Effect in Liquid Crystal Networks: A General Approach for Self-Sustained Mechanical Oscillators. *Adv. Mater.* **2017**, 29, 1606712.

(28) Mirvakili, S. M.; Hunter, I. W. Artificial Muscles: Mechanisms, Applications, and Challenges. *Adv. Mater.* **2018**, 30, 1704407.

(29) Hu, J.; Wang, W.; Yu, H. Endowing Soft Photo-Actuators with Intelligence. *Adv. Intell. Syst.* **2019**, 1, 1900050.

(30) Van Oosten, C. L.; Corbett, D.; Davies, D.; Warner, M.; Bastiaansen, C. W. M. M.; Broer, D. J. Bending Dynamics and Directionality Reversal in Liquid Crystal Network Photoactuators. *Macromolecules* **2008**, 41, 8592−8596.

(31) Zeng, H.; Wasylczyk, P.; Wiersma, D. S.; Priimagi, A. Light Robots: Bridging the Gap between Microrobotics and Photomechanics in Soft Materials. *Adv. Mater.* **2018**, 30, 1703554.

(32) Jiang, Z. C.; Xiao, Y. Y.; Zhao, Y. Shining Light on Liquid Crystal Polymer Networks: Preparing, Reconfiguring, and Driving Soft Actuators. *Adv. Opt. Mater.* **2019**, 7, 1900262.

(33) McBride, M. K.; Martinez, A. M.; Cox, L.; Alim, M.; Childress, K.; Beiswinger, M.; Podgorski, M.; Worrell, B. T.; Killgore, J.; Bowman, C. N. A Readily Programmable, Fully Reversible Shape-Switching Material. *Sci. Adv.* **2018**, 4, No. eaat4634.

(34) McBride, M. K.; Hendrikx, M.; Liu, D.; Worrell, B. T.; Broer, D. J.; Bowman, C. N. Photoinduced Plasticity in Cross-Linked Liquid Crystalline Networks. *Adv. Mater.* **2017**, 29, 1606509.

(35) Ube, T.; Kawasaki, K.; Ikeda, T. Photomobile Liquid-Crystalline Elastomers with Rearrangeable Networks. *Adv. Mater.* **2016**, 28, 8212−8217.

(36) Wang, Z.; Tian, H.; He, Q.; Cai, S. Reprogrammable, Reprocessible, and Self-Healable Liquid Crystal Elastomer with Exchangeable Disulfide Bonds. *ACS Appl. Mater. Interfaces* **2017**, 9, 33119−33128.

(37) Jiang, Z.; Xiao, Y.; Yin, L.; Han, L.; Zhao, Y. Self-Lockable" Liquid Crystalline Diels−Alder Dynamic Network Actuators with Room Temperature Programmability and Solution Reprocessability. *Angew. Chem.* **2020**, 132, 4955−4961.

(38) Jiang, Z. C.; Xiao, Y. Y.; Tong, X.; Zhao, Y. Selective Decrosslinking in Liquid Crystal Polymer Actuators for Optical Reconfiguration of Origami and Light-Fueled Locomotion. *Angew. Chem., Int. Ed.* **2019**, 58, 5332−5337.

(39) Lahikainen, M.; Zeng, H.; Priimagi, A. Reconfigurable Photoactuator through Synergistic Use of Photochemical and Photothermal Effects. *Nat. Commun.* **2018**, 9, 4148.

(40) Nie, H.; Self, J. L.; Kuenstler, A. S.; Hayward, R. C.; Read de Alaniz, J. Multiaddressable Photochromic Architectures: From Molecules to Materials. *Adv. Opt. Mater.* **2019**, 7, 1900224.

(41) Goulet-Hanssens, A.; Eisenreich, F.; Hecht, S. Enlightening Materials with Photoswitches. *Adv. Mater.* **2020**, 32, 1905966.

(42) Van Oosten, C. L.; Bastiaansen, C. W. M.; Broer, D. J. Printed Artificial Cilia from Liquid-Crystal Network Actuators Modularly Driven by Light. *Nat. Mater.* **2009**, 8, 677−682.

(43) Yu, Y.; Nakano, M.; Ikeda, T. Directed Bending of a Polymer Film by Light. *Nature* **2003**, 425, 145.

(44) Iamsaard, S.; Anger, E.; Aßhoff, S. J.; Depauw, A.; Fletcher, S. P.; Katsonis, N. Fluorinated Azobenzenes for Shape-Persistent Liquid Crystal Polymer Networks. *Angew. Chem., Int. Ed.* **2016**, 55, 9908−9912.

(45) Ryabchun, A.; Li, Q.; Lancia, F.; Aprahamian, I.; Katsonis, N. Shape-Persistent Actuators from Hydrazone Photoswitches. *J. Am. Chem. Soc.* **2019**, 141, 1196−1200.

(46) Herder, M.; Schmidt, B. M.; Grubert, L.; Pätzel, M.; Schwarz, J.; Hecht, S. Improving the Fatigue Resistance of Diarylethene Switches. *J. Am. Chem. Soc.* **2015**, 137, 2738−2747.

(47) Frigoli, M.; Welch, C.; Mehl, G. H. Design of Mesomorphic Diarylethene-Based Photochromes. *J. Am. Chem. Soc.* **2004**, 126, 15382−15383.

(48) Leydecker, T.; Herder, M.; Pavlica, E.; Bratina, G.; Hecht, S.; Orgiu, E.; Samorì, P. Flexible Non-Volatile Optical Memory Thin-Film Transistor Device with over 256 Distinct Levels Based on an Organic Bicomponent Blend. *Nat. Nanotechnol.* **2016**, 11, 769−775.

(49) Van Oosten, C. L.; Harris, K. D.; Bastiaansen, C. W. M.; Broer, D. J. Glassy Photomechanical Liquid-Crystal Network Actuators for Microscale Devices. *Eur. Phys. J. E: Soft Matter Biol. Phys.* **2007**, 23, 329−336.

(50) De Haan, L. T.; Schenning, A. P. H. J.; Broer, D. J. Programmed Morphing of Liquid Crystal Networks. *Polymer* **2014**, 55, 5885−5896.

(51) Van Nostrum, C. F.; Nolte, R. J. M.; Broer, D. J.; Fuhrman, T.; Wendorff, J. H. Photoinduced Opposite Diffusion of Nematic and Isotropie Monomers during Patterned Photopolymerization. *Chem. Mater.* **1998**, 10, 135−145.

(52) Mamiya, J. I.; Kuriyama, A.; Yokota, N.; Yamada, M.; Ikeda, T. Photomobile Polymer Materials: Photoresponsive Behavior of Cross-Linked Liquid-Crystalline Polymers with Mesomorphic Diarylethenes. *Chem. - Eur. J.* **2015**, 21, 3174−3177.

(53) Irie, M.; Fukaminato, T.; Matsuda, K.; Kobatake, S. Photochromism of Diarylethene Molecules and Crystals: Memories, Switches, and Actuators. *Chem. Rev.* **2014**, 114, 12174−12277.

(54) Kumar, K.; Schenning, A. P. H. J.; Broer, D. J.; Liu, D. Regulating the Modulus of a Chiral Liquid Crystal Polymer Network by Light. *Soft Matter* **2016**, 12, 3196−3201.

(55) Shimamura, A.; Priimagi, A.; Mamiya, J.; Ikeda, T.; Yu, Y.; Barrett, C. J.; Shishido, A. Simultaneous Analysis of Optical and Mechanical Properties of Cross-Linked Azobenzene-Containing Liquid-Crystalline Polymer Films. *ACS Appl. Mater. Interfaces* **2011**, 3, 4190−4196.

(56) Lancia, F.; Ryabchun, A.; Nguindjel, A. D.; Kwangmettatam, S.; Katsonis, N. Mechanical Adaptability of Artificial Muscles from Nanoscale Molecular Action. *Nat. Commun.* **2019**, *10*, 4819.

(57) Yamada, M.; Kondo, M.; Mamiya, J. I.; Yu, Y.; Kinoshita, M.; Barrett, C. J.; Ikeda, T. Photomobile Polymer Materials: Towards Light-Driven Plastic Motors. *Angew. Chem., Int. Ed.* **2008**, *47*, 4986−4988.

(58) Kumar, K.; Knie, C.; Bléger, D.; Peletier, M. A.; Friedrich, H.; Hecht, S.; Broer, D. J.; Debije, M. G.; Schenning, A. P. H. J. H. J. A Chaotic Self-Oscillating Sunlight-Driven Polymer Actuator. *Nat. Commun.* **2016**, *7*, 11975.

(59) Vantomme, G.; Gelebart, A. H.; Broer, D. J.; Meijer, E. W. A Four-Blade Light-Driven Plastic Mill Based on Hydrazone Liquid-Crystal Networks. *Tetrahedron* **2017**, *73*, 4963−4967.

(60) Lan, R.; Sun, J.; Shen, C.; Huang, R.; Zhang, Z.; Ma, C.; Bao, J.; Zhang, L.; Wang, L.; Yang, D.; Yang, H. Light-Driven Liquid Crystalline Networks and Soft Actuators with Degree-of-Freedom-Controlled Molecular Motors. *Adv. Funct. Mater.* **2020**, *30*, 2000252.

(61) Gelebart, A. H.; Mulder, D. J.; Vantomme, G.; Schenning, A. P. H. J.; Broer, D. J. A Rewritable, Reprogrammable, Dual Light-Responsive Polymer Actuator. *Angew. Chem., Int. Ed.* **2017**, *56*, 13436−13439.

(62) Gimenez-Pinto, V.; Ye, F.; Mbanga, B.; Selinger, J. V.; Selinger, R. L. B. Modeling Out-of-Plane Actuation in Thin-Film Nematic Polymer Networks: From Chiral Ribbons to Auto-Origami Boxes via Twist and Topology. *Sci. Rep.* **2017**, *7*, 45370.

(63) Kobatake, S.; Takami, S.; Muto, H.; Ishikawa, T.; Irie, M. Rapid and Reversible Shape Changes of Molecular Crystals on Photo-irradiation. *Nature* **2007**, *446*, 778−781.

(64) Kitagawa, D.; Tsujioka, H.; Tong, F.; Dong, X.; Bardeen, C. J.; Kobatake, S. Control of Photomechanical Crystal Twisting by Illumination Direction. *J. Am. Chem. Soc.* **2018**, *140*, 4208−4212.

(65) Preston, D. J.; Rothemund, P.; Jiang, H. J.; Nemitz, M. P.; Rawson, J.; Suo, Z.; Whitesides, G. M. Digital Logic for Soft Devices. *Proc. Natl. Acad. Sci. U. S. A.* **2019**, *116*, 7750−7759.

(66) Duncan, P. N.; Nguyen, T. V.; Hui, E. E. Pneumatic Oscillator Circuits for Timing and Control of Integrated Microfluidics. *Proc. Natl. Acad. Sci. U. S. A.* **2013**, *110*, 18104−18109.

(67) Zhang, X.; Soh, S. Performing Logical Operations with Stimuli-Responsive Building Blocks. *Adv. Mater.* **2017**, *29*, 1606483.

(68) Qi, Z.; Malo De Molina, P.; Jiang, W.; Wang, Q.; Nowosinski, K.; Schulz, A.; Gradzielski, M.; Schalley, C. A. Systems Chemistry: Logic Gates Based on the Stimuli-Responsive Gel-Sol Transition of a Crown Ether-Functionalized Bis(Urea) Gelator. *Chem. Sci.* **2012**, *3*, 2073−2082.

(69) Komatsu, H.; Matsumoto, S.; Tamaru, S.-i.; Kaneko, K.; Ikeda, M.; Hamachi, I. Supramolecular Hydrogel Exhibiting Four Basic Logic Gate Functions to Fine-Tune Substance Release. *J. Am. Chem. Soc.* **2009**, *131*, 5580−5585.